Bulgarian Chemical Communications, Volume 47, Number 4 (pp. 1045 – 1052) 2015

Silver nanoparticle forms with new organometallic compounds enhance antimicrobial activities

E. A. El-Sawi*, M. A. Hosny

Department of Chemistry, Faculty of Women for Arts, Science and Education
Ain Shams University, Heliopolis, Cairo, Egypt

Received January 6, 2015, Revised July 30, 2015

Metallated heterocyclic compounds (4-9) were obtained from the reaction of 2-(2-oxo-2*H*-pyrano[3,2-*h*] quinolin-4-yl) acetic acid (1) and 4-(2,2-dihydroxy-vinyl)-2*H*-pyrano[3,2-*h*] quinolin-2-one (2) and their derivative (3) with Co(II) and Cu(II) acetates. Elucidation of the structures were based on their elemental analyses, IR, ^{1}HNMR, and MS. The prepared silver nanoparticles were confirmed by transmission electron microscopy (TEM) and UV spectra. The antimicrobial activities of the all products with their silver nanoparticle forms were investigated to compare their effect with respect to the parent new compounds. The results indicated that silver nanoparticles increased by 12-170% and can be used as effective growth inhibitors for microorganism.

Key words: pyrano-quinoline-metallation-antimicrobial- Silver nanoparticles.

INTRODUCTION

The antimicrobial activity of silver nanoparticles (Ag-NPs), gold nanoparticles and platinum nanoparticles (Pt-NPs) in aqueous solution were investigated. The minimum inhibitory concentration (MIC) of (Ag-NPs) for *S.aureus* and *E.coli* were 5 and 10 ppm, respectively, but the (Au-NPs) stabilized with sodium dodecylsulfate (SDS) did not show antimicrobial activity. Also the (Pt-NPs) stabilized with poly-(N-vinyl-2-pyrrolidone) (PVP) or (SDS) did not show antimicrobial activity for the test organisms [1]. Silver had been in use in the form of metallic silver, silver nitrate, silver sulfadiazine for the treatment of burns, wounds, several bacterial infections and metallic silver in the form of silver nanoparticles had made a remarkable comeback as a potential antimicrobial agent [2]. Jiang et al. [3] reported that gold and silver nanoparticles coated with antibodies can regulate the process of membrane receptor internalization. The silver nanoparticles were found to accumulate in the bacterial membrane.

A membrane with such morphology exhibited a significant increase in permeability, resulting in death of the cell [4]. The antimicrobial activity of silver nanoparticles was investigated against yeast, *Escherichia coli*, and *Staphylococcus aureus* [5]. Quinolines form an interested and important group of compounds; they possess excellent application for their pharmacological properties. Quinoline derivatives 2-(2-oxo-2*H*-pyrano[3,2-*h*]quinolin-4-yl) acetic acid , 4-(2,2- dihydroxy-vinyl)-2*H*-pyrano[3,2-*h*]quinolin-2-one, their derivatives obtained via their reactions with N-(2-amino ethyl) propane-1,3-diamine and their palladated products exhibited antimicrobial activity as well as their silver nanoparticle forms also some exhibit anticancer activity against breast cancer [6]. Quinolines showed antimicrobial [7], antimalarial [8], anti-inflammatory [9], antitumor [10], antioxidant [11], and antiplatelet [12] activity. Pyranoquinoline also showed antimicrobial activities [13]. Many derivatives of this heterocyclic compounds are biologically active and are found to be useful intermediates for many medicinal products [14], [15], as well as derivatives containing pyrazole and indoline moieties have excellent antibacterial and antifungal activities [16]. Schiff base 2-(4-methoxybenzylidene amino) benzene-thiol, its metallation with mercury (II), nickel (II), palladium (II) gave compounds exhibited antimicrobial and anticancer activity [17]. Organo-mercury compounds via metallation of some new Schiff bases were also synthesized [18], [19].

In continuation to our previous work the study was directed to synthesize new organometallic compounds containing Co (II) and Cu (II) to study the effect of silver nanoparticles on their antimicrobial activity.

RESULTS AND DISCUSSION

New compounds (4) and (5) were obtained from the reactions of compounds 2-(2-oxo-2*H*-pyrano[3,2-*h*] quinolin-4-yl) acetic acid (1) and 4-

* To whom all correspondence should be sent:
E-mail: elsawi_e@yahoo.com

(2,2- dihydroxy-vinyl)-2*H*-pyrano[3,2-*h*] quinolin-2-one (2) [6] with cobalt acetate. The reactions may proceed as follows, cf. Scheme (1).

Elucidation of the structures based on their elemental analyses, IR, ^{1}HNMR and MS spectra. The IR spectra showed ν_{OH} at 3424 cm^{-1} , $\nu_{C=O}$ for carboxylate attached to cobalt at 1610 cm^{-1} (antisymmetrical) & 1420 cm^{-1} (symmetrical stretching) , $\nu_{Co\text{-}C}$ at 536 cm^{-1} and $\nu_{Co\text{-}o}$ at 458 cm^{-1} for compound (4), and broad absorption band at 3650- 2600 cm^{-1}for ν_{OH} & at 1710 cm^{-1} for $\nu_{C=O}$ due to carboxylic group and $\nu_{Co\text{-}C}$ at 529 cm^{-1} and $\nu_{Co\text{-}C}$ at 469 cm^{-1} for compound (5).

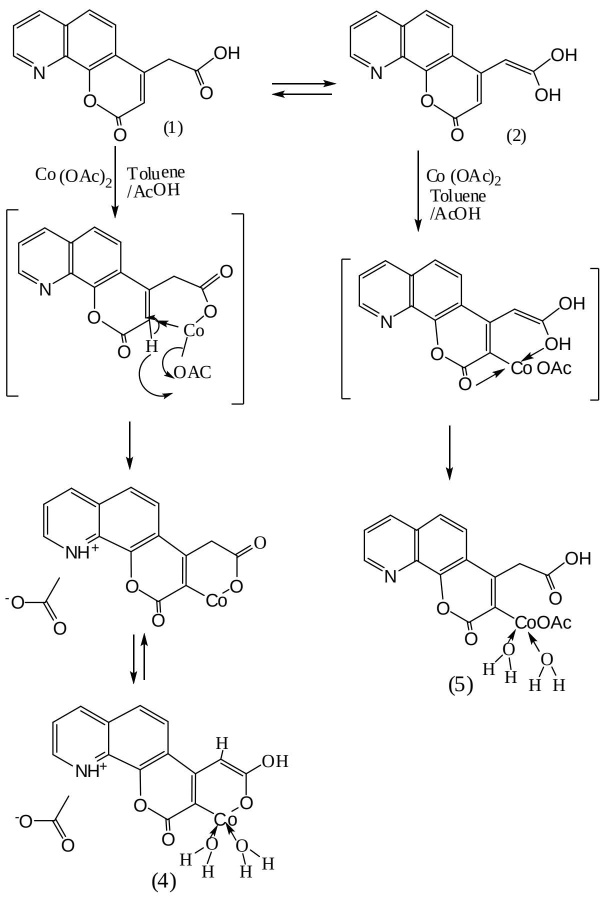

Scheme 1.

The ^{1}HNMR spectrum for compound (4) showed δ 11.93 ppm (1H, for OH), δ 9.46 - 7.01 ppm (5H, for aromatic protons) and δ 6.8 ppm (1H, for methine proton) and δ 2.20 ppm (3H, for methyl protons). The ^{1}HNMR spectrum for compound (5) showed δ 12.0 ppm (1H,for OH), δ 8.40-7.01 ppm (5H, for aromatic protons) and δ 2.80 ppm (2H, for methylene protons).

The MS spectra for compounds (4) & (5) showed $M^{+\cdot}$ at m/z 372 (40.60%), the base peak at 57 (100%) can be attributed to $C_3H_7N^{+\cdot}$ & $M+1^{+}$ at m/z 373 (1.02 %)) the base peak at 370 (100%). can be attributed to $M\text{-}2^{+}$. Compounds (6) and (7) were obtained from the reactions of compounds (1) and (2) with copper acetate. The reactions may proceed as follows cf. Scheme (2). The structures were inferred from their elemental analyses, IR, ^{1}HNMR and MS spectra. The IR spectrum for compounds(6) showed ν_{OH} at 3394 cm^{-1}, $\nu_{C=O}$ for carboxylate ion at 1610 cm^{-1} (antisymmetrical) & 1405 cm^{-1} (symmetrical stretching)and $\nu_{Cu\text{-}C}$ at 577 cm^{-1} , while compound (7) showed two absorption bands at 3500& 3398 cm^{-1} for two ν_{OH} & at 1633 cm^{-1} for $\nu_{C=O}$ due to carboxylic group and $\nu_{Cu\text{-}C}$ at 580 cm^{-1}.

The ^{1}HNMR spectrum for compound (6) showed δ 11.90 ppm (1H, for OH), δ 9.50- 7.45 ppm (5H, for aromatic protons) and δ 6.27 ppm (1H, for methane proton) and δ 2.39 ppm (3H, for methyl protons).

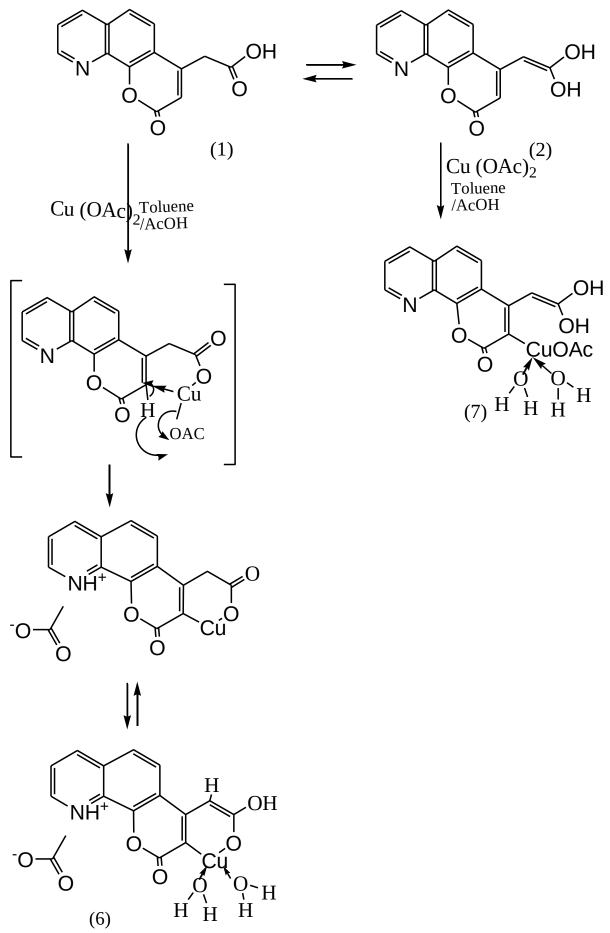

Scheme 2.

The ^{1}HNMR spectrum for compound (7) showed δ 11.84 ppm (2H, for2 OH), δ 9.79-7.04 ppm (5H, for aromatic protons), δ 6.44 ppm (1H, for methine proton) and δ 2.28 ppm (3H, for CH_3).

The MS spectrum for compounds (6) showed M at m/z 377 (24.53%), the base peak at 353 (100%) can be attributed to $M\text{-}24]^{+}$ and the MS spectrum for (7) showed M at m/z 377(8.97 %)) the base peak at 69 (100%) can be attributed to $C_4H_7N]^{+}$.

Metallation of compound (3) [6] with cobalt acetate and copper acetate.

The metallation of compound (3) [6] with cobalt acetate and copper acetate gave rise to new metallated compounds (8) and (9) via coordination to nitrogen then followed by electrophilic substitution in the o-position cf. Scheme (3).

Elucidation of the structure of compound (8) based on IR, ^{1}HNMR and MS spectra. The IR spectrum showed new absorption bands two bands for ν_{NH2} at 3494, 3420 cm^{-1}, ν_{NH} at 3321 cm^{-1} ,ν_{CHstr} at 2953 cm^{-1}, $\nu_{C=O}$ at 1653 cm^{-1}, $\nu_{C=C\ Alken}$ at 1614 cm^{-1}, $\nu_{C\text{-}H\ bending}$ at 1463 cm^{-1} , $\nu_{C\text{-}Co}$ at 548 cm^{-1}, $\nu_{O\text{-}Co}$ at 463 cm^{-1}. The ^{1}HNMR spectrum showed δ 7.8-6.67 ppm (4H, for aromatic protons), δ 6.63ppm (1H, for=C-H proton), δ 3.96 ppm (1H, for O-C-C= CH proton), δ 2.7, 2.8 ppm (4H, for2 CH_2 protons attached to NH and NH_2), δ 1.6, 2.3, 2.6 ppm (6 H, for 3CH_2 protons), δ2.1 ppm (3H, for 3 OH protons). The absence of 8.9 ppm indicated that substitution reaction took place at this position via coordination with N in the pyridine ring followed by electrophilic substitution in the aromatic moiety.The MS spectra showed the M+2 at m/z 431(1.25%) and the base peak at m/z 108(100%) due to 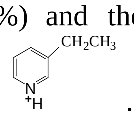 .

The IR spectrum of compound (9) indicated the presence of new absorption bands for ν_{NH2} two bands at 3493,3419 cm^{-1}, $\nu_{C=O}$ at 1657 cm^{-1}, $\nu_{C\text{-}Cu}$ at 549 cm^{-1} and $\nu_{O\text{-}Cu}$ at 463 cm^{-1}. The ^{1}HNMR spectrum showed δ 7.8-7.2 ppm (4H, for aromatic protons), δ 6.70 ppm (1H, for =C-H proton), δ 4.3 ppm (1H, for O-C-C= CH proton), δ 2.7, 2.9 and 3.2 ppm (4H, for2 CH_2 protons attached to NH and NH_2 , and 4H for 2CH_2 attached to N-C=O), δ2.1 ppm (3H, for 3 OH protons) [20] and δ 1.8 ppm (2 H, for CH_2 protons). The MS spectrum showed the $M+1]^{+}$ at m/z 435 (36.32%) and the base peak at m/z 108(100%) due to 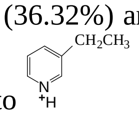 .

BIOLOGICAL ACTIVITY

Measurement of Antimicrobial Activity using Diffusion disc Method

A filter paper sterilized disc saturated with measured quantity of the sample is placed on a plate containing solid bacterial medium (nutrient agar broth) or fungal medium (Doxs medium) which has been heavily seeded with the spore suspension of the tested organism. After incubation, the diameter of the clear zone of inhibition surrounding the sample is taken as a measure of the inhibitory power of the sample against the particular test organism [21-24].

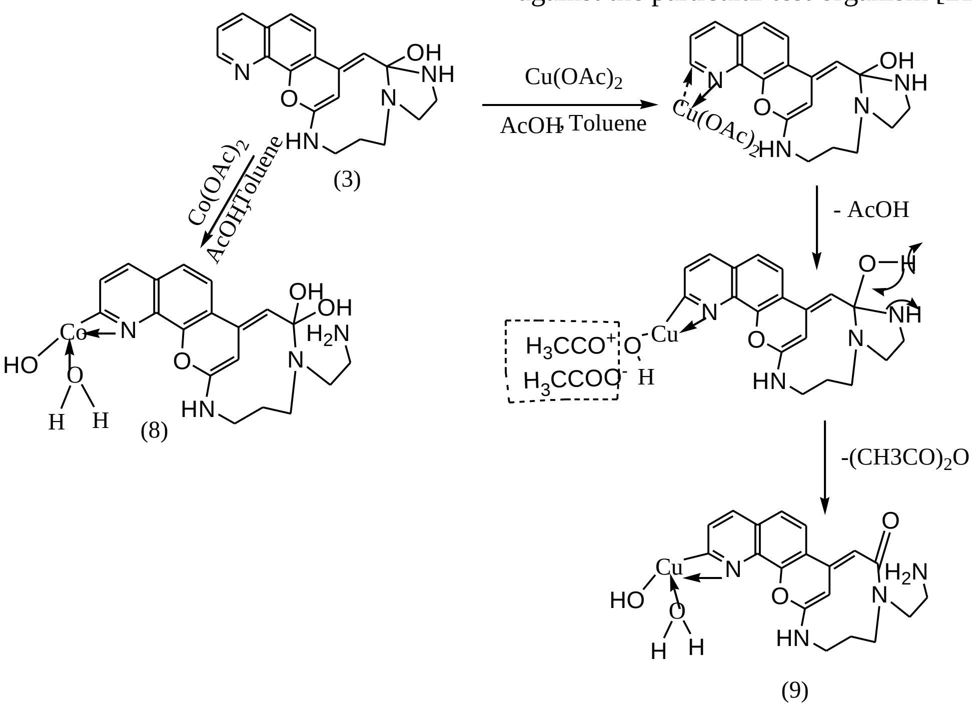

Sheme 3.

Table 1. The antimicrobial activities of the compounds (5-8 & 10-11) and their silver nano-forms.

Compds. No.	Candida albicans	Fold increase% (nano.-parent)/ parent X100=	Aspergi-llus Niger	Fold increase% (nano.-parent)/ parent X100=	Staphylo-coccus aureus (G+)	Fold increase% (nano-parent)/ parent X100=	Escheri-chia coli (G-)	Fold increase% (nano.-parent)/ parent X100=
Inhibition zone in mm (conc.µg/ml)								
Tetracycline Antibacterial	------		------		20		22	
Amphotericin Antifungal	20		20		------		------	
4	14	71.42	11	102.09	0.0		0.0	
4 nano-form	24		23		22		22	
5	26	23.07	26	23.07	27	22.22	27	22.22
5 nano-form	32		32		33		33	
6	19	52.63	18	61.11	14	85.71	8	225
6 nano-form	29		29		26		26	
7	25	12	25	12	25	16	25	16
7 nano-form	28		28		29		29	
8	23	34.78	22	40.90	23	39.13	22	45.45
8 nano-form	31		31		32		32	
9	10	170	11	145.45	12	133.33	14	100
9 nano-form	27		27		28		28	

Weakly active: less than 10mm, Moderately active: 10-20 mm, Highly active: 20-25 mm, Strong active: more than 25 mm

The antimicrobial activities of all compounds were tested. Compound (5) showed strong activity towards bacteria and fungi under investigation and compounds (7) and (8) showed high activity. The effect of silver nanoparticles on the biological activity efficiency was investigated using chemical reduction method [25-28]. TEM and SEM images of silver nanoparticle are shown in Fig. 1a and Fig. 1b and TEM for nanoforms of compounds (5), (7), (8) and (9) are shown in Figures 2a, 3a, 4 and 5. The SEM images for the nanoforms of compounds (5),(8) are shown in Fig. 2b and Fig. 3b. Generally the nanoforms of compounds (5-9) exhibit strong activities and the nanoform of compound (4) showed high activity. The highest fold increases in area were observed for (9) in presence of Ag-NPs solution against *Candida albicans*, *Aspergillus Niger* and *Staphylococcus aureus* (G+), and the highest fold increases in area were observed for(6) in presence of Ag-NPs solution against *Escherichia coli*(G-) Table 1.

Transmission electron microscopy (TEM) and (SEM) images of the Ag-NPs solution and the Ag-NPs of the compound (4) and (5)

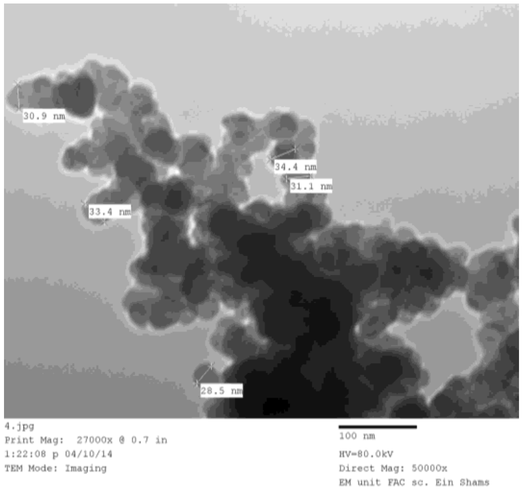

Fig. 1a. TEM Ag-NPs.

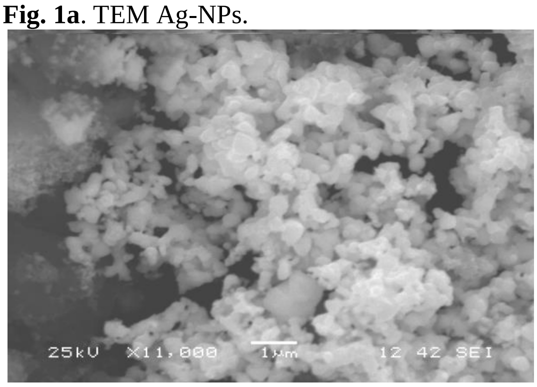

Fig.1b. SEM Ag –NPs.

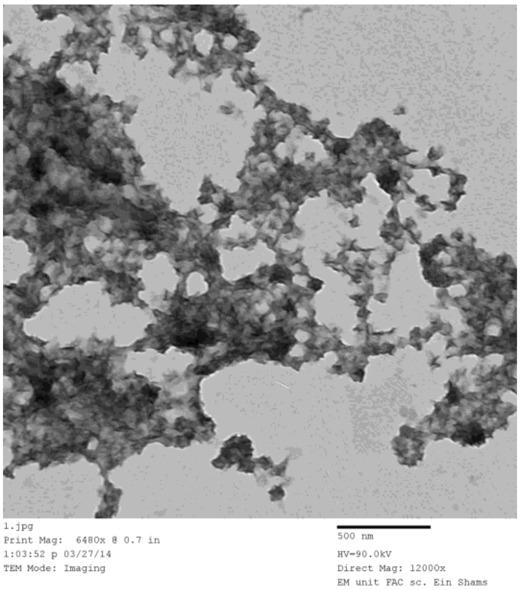

Fig. 2a. TEM micrograph of compound (5).

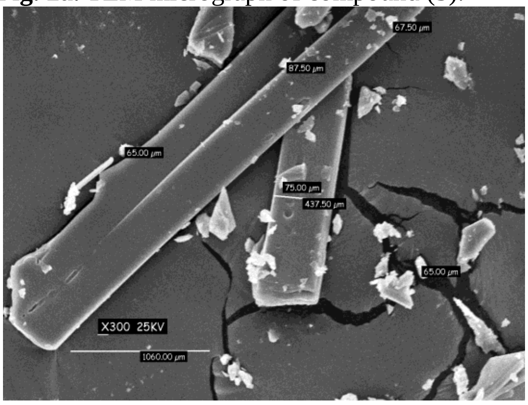

Fig. 2b. SEM of compound (5) after addition of Ag-NPs solution,after addition of Ag-NPs solution
Scale bar = 100 µm

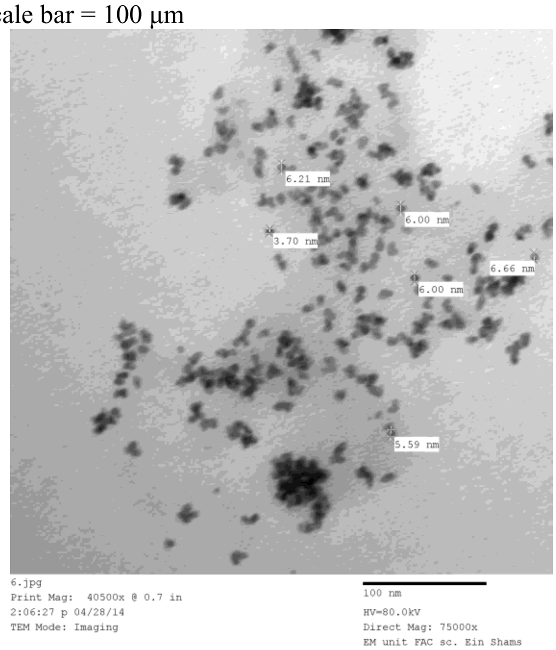

Fig. 3a. TEM micrograph of compound (8) after addition of Ag-NPs solution, Scale bar = 100 µm,

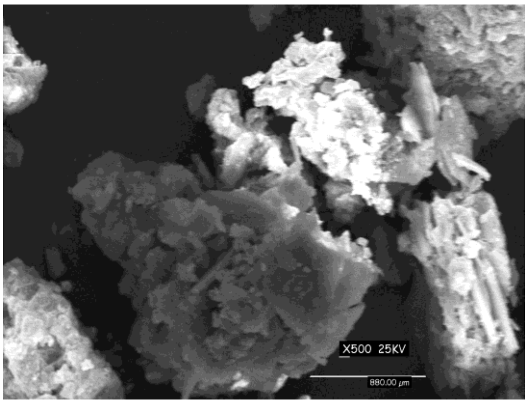

Fig. 3b. SEM of compound (8) after addition of Ag-NPs solution

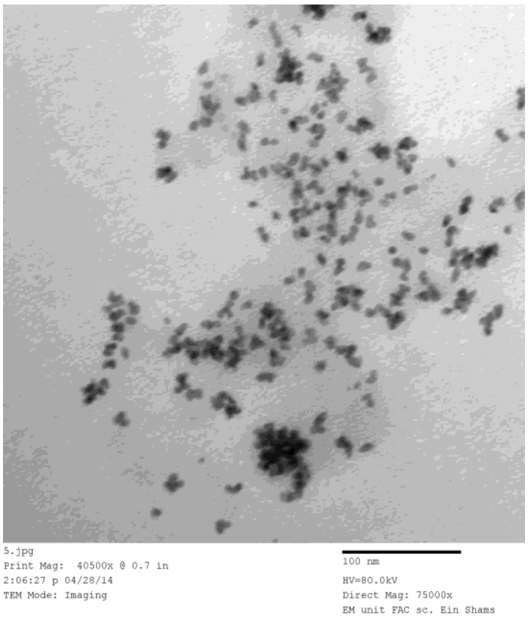

Fig. 4. TEM micrograph of compound (7) after addition of Ag- NPs solution.

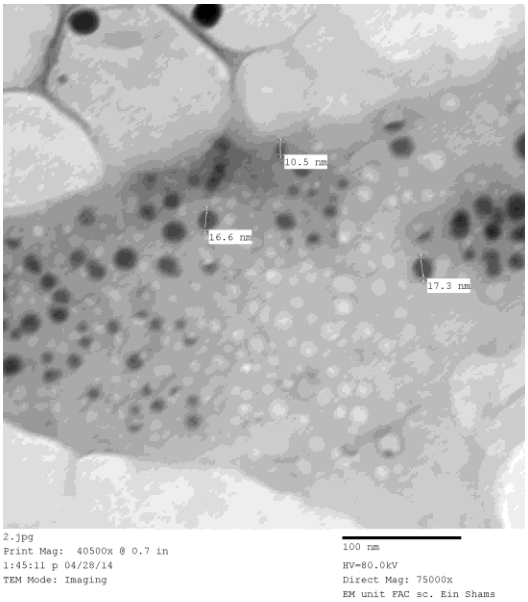

Fig. 5. TEM of compound (9) after addition of Ag-NPs solution.

EXPERIMENTAL

Melting points were measured by a Gallen Kamp melting point apparatus. Thin layer chromatography was performed with fluorescent silica gel plates HF254 (Merck), and plates were viewed under UV light at 254 and 265 nm. Infrared spectra (ν cm^{-1}) were recorded on Bruker Vector Germany and on Mattson FT-IR 1000, using KBr disks. Mass spectra were measured on GCQ Finnigan MAT in Micro Analytical Centre, Cairo University, Giza, Egypt. 1H-NMR spectra were recorded on Gemini 200 MHZ NMR spectrometer, in DMSO-d6 solution with TMS as internal standard. It was determined in microanalytical centre in main defence chemical laboratory of the Egyptian Accreditation council. The antibacterial activity was determined in microanalytical center in main defence chemical laboratory of the Egyptian Accreditation Council. Transmission electron microscopy (TEM) images and scanning electron microscopy (SEM) were taken on (JEOL; model 1200 EX) at an accelerator voltage of 80 kV, in Central lab., Ain Shams University.

Metallation of compound (1a),(1b)& (2b) with cobalt acetate and copper acetate

General Procedure

The cobalt or nickel acetate (1mmol) reacts with (1a) or (1b) & or (2b) [6] (1mmol) in 50 mL of toluene in the presence of few drops of acetic acid under reflux for 3h. The precipitated crystals (compounds 4-9) are filtered, dried, and crystallized from acetic acid.

Compound (4): Pale brownish white crystals, (yield: 85 %), m.p.340-341 ^oC, IR (KBr) (cm^{-1}): showed ν_{OH} at 3424, $\nu_{C=O}$ for carboxylate (attached to cobalt) at 1635 (antisymmetrical) & 1420 (symmetrical stretching) and 536 and 458 for ν_{Co-C} and ν_{Co-o} respectively. The ^{1}HNMR spectrum for compound (4) showed δ 11.93 ppm (1H,for OH), δ 9.46- 7.01 ppm (5H, for aromatic protons) and δ 6.8 ppm (1H, for methine proton) and δ 2.20 ppm (3H, for methyl protons). The MS spectrum showed the molecular ion peak $M]^{+\cdot}$ at m/z 372 (40.60%) the base peak at 57 (100%) can be attributed to $C_3H_7N]^{+\cdot}$

Compound (5): Pale brownish crystals, (yield: 86 %), m.p. d.240 ^oC, IR (KBr) (cm^{-1}): at 1710 cm^{-1} for $\nu_{C=O}$ due to carboxylic group, 529 and 469 for ν_{Co-C} and and ν_{Co-O}. The ^{1}HNMR spectrum for compound (5) showed δ 12.0 ppm (1H,for OH), δ 8.40-7.01 ppm (5H, for aromatic protons) and δ 2.80 ppm (2H, for methylene protons). The MS spectrum showed $M+1]^{+}$ at m/z 372(1.02%), the base peak at 370 (100%) can be attributed to $M-2]^{+}$.

Compound (6): Pale brownish white crystals, (yield: 81 %), m.p.d.340 ^oC, IR (KBr) (cm^{-1}): showed ν_{OH} at 3394 cm^{-1}, $\nu_{C=O}$ for carboxylate ion at 1610 cm^{-1} (antisymmetrical) &1405 cm^{-1} (symmetrical stretching)and ν_{Cu-C} at 577 cm^{-1} The ^{1}HNMR spectrum for compound (6) showed δ 11.90 ppm (1H,for OH), δ 9.50- 7.45 ppm (5H, for aromatic protons) and δ 6.27 ppm (1H, for methane proton) and δ 2.39 ppm (3H, for methyl protons). The MS spectrum showed $M]^{+\cdot}$ at m/z 377(24.53%), the base peak at 353 can be attributed to $M-24]^{+}$

Compound (7): Pale brownish white crystals, (yield: 83 %), m.p.120-121 ^oC, IR (KBr) (cm^{-1}): showed two absorption bands at 3500& 3398 cm^{-1} for two ν_{OH} &at 1633 cm^{-1} for $\nu_{C=O}$ due to carboxylate ion. The ^{1}HNMR spectrum for compound (7) showed δ 11.84 ppm (2H, for 2 OH), δ 9.79-7.04 ppm (5H, for aromatic protons), δ 6.44 ppm (1H, for methine proton) and δ 2.28 ppm (3H, for CH_3). The MS spectrum showed $M]^{+\cdot}$ at m/z 377(8.97 %)) and the base peak at 69 (100%) can be attributed to $C_4H_7N]^{+}$

Compound (8): Pale brownish white crystals, (yield: 71 %), m.p.250-251 ^oC, IR (KBr) (cm^{-1}): showed new absorption bands: two bands for ν_{NH2} at 3494, 3420 cm^{-1}, ν_{NH} at 3321 cm^{-1} ,ν_{CHstr} at 2953 cm^{-1}, $\nu_{C=O}$ at 1653 cm^{-1}, $\nu_{C=C\ Alkene}$ at 1614 cm^{-1}, $\nu_{C-H\ bending}$ at 1463 cm^{-1} , ν_{C-Co} at 548 cm^{-1}, ν_{O-Co} at 463 cm^{-1}. ^{1}HNMR spectrum showed δ 7.8-6.67 ppm(4H, for aromatic protons), δ 6.63ppm (1H,for =C-H proton), δ 3.96 ppm(1H,for O-C-C= CH proton), δ 2.7, 2.8 ppm (4H, for2 CH_2 protons attached to NH and NH_2), δ 1.6, 2.3, 2.6 ppm (6 H, for 3CH_2 protons), δ2.1 ppm (3H, for 3 OH protons).The absence of 8.9 ppm indicated that substitution reaction took place at this position via coordination with N in the pyridine ring followed by electrophilic substation in the aromatic moiety. The MS spectra showed the $M+2]^{+\cdot}$ at m/z 431(1.25%) and the base peak at m/z 108(100%) attributed to 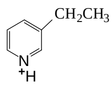

.

Compound (9): brownish crystals, (yield: 70 %), m.p.184-185 ^oC, IR (KBr) (cm^{-1}): The IR spectrum indicated the presence of new absorption bands for ν_{NH2} two bands at 3493, 3419 cm^{-1}, $\nu_{C=O}$ at 1657

cm^{-1}, $\nu_{C\text{-}Cu}$ at 549 cm^{-1} and $\nu_{O\text{-}Cu}$ at 463 cm^{-1}. The ^{1}HNMR spectrum showed δ 7.8-7.2 ppm (4H,for aromatic protons), δ 6.70 ppm (1H,for =C-H proton), δ 4.3 ppm (1H, for O-C-C= CH proton), δ 2.7, 2.9 and 3.2 ppm (4H, for2 CH_2 protons attached to NH and NH_2 ,and 4H for 2CH_2 attached to N-C=O), δ2.1 ppm (3H, for 3 OH protons) [20] and δ 1.8 ppm (2 H, for CH_2 protons). The MS spectrum showed the $[M+1]^+$ at m/z 435(36.32%) and the base peak at m/z 108(100%) due to

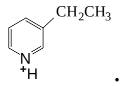

.

Preparation of silver nanoparticles:

Silver nanoparticles were prepared by chemical reduction method [28]. All solutions were prepared in distilled water. 50 ml of 0.001 M silver nitrate was heated to boiling using hot plate magnetic stirrer. To this solution 5 ml of 1% trisodium citrate was added drop by drop. During this process solution was mixed vigorously. Solution was heated until colour change is evident (yellowish brown). Then it was removed from the heating element and stirred until cool to room temperature. UV/Visible spectrum for the silver nanoparticles in the solution showed λ max at 420 nm due to the surface plasmon resonance effect.

CONCLUSION

Metallated heterocyclic compounds (4-9) were synthesized from the reaction of 2-(2-oxo-2*H*-pyrano[3,2-*h*]quinolin-4-yl) acetic acid (1) and 4-(2,2-dihydroxy-vinyl)-2*H*-pyrano[3,2-*h*]quinolin-2-one (2) and their derivative (3) with Co(II) and Cu(II) acetates. The antimicrobial activities of the all products and their silver nanoparticle forms were examined. The antibacterial and antifungal activities of the silver nano forms (Ag-NPs) of the compounds were screened to compare their effect with respect to the parent new compounds. Compound (5) showed strong activity towards bacteria and fungi under investigation and compounds (7) and (8) showed high activity. The nanoforms of compounds (5-9) exhibit strong activities and the nanoform of compound (4) showed high activity. The highest fold increases in area were observed for (9) in presence of Ag-NPs solution against *Candida albicans*, Aspergillus Niger and staphylococcus aureus (G+), and the highest fold increases in area were observed for (6) in presence of Ag-NPs solution against escherichia coli (G-) Table 1.

Acknowledgements: *The authors would like to thank the Chemistry Department, Faculty of Women, Ain Shams University in conducting and supporting this research.*

REFERENCES

1.K. H. Cho, J. E. Park, T. Osaka, S. G. Park, *Electrochimica Acta*, **51**: 956 (2005).

2.M. Rai, A. Yadav, A. Gade, *Biotechnology Advan*ces, **27,** 76 (2009).

3.W. Jiang, B. Y. S Kim., J. T. Rutka, C. W. Chan Warren, *Nature Nanotechnology*, **3**, 145 (2008).

4.I.Sondi, B. Salopek-Sond., *Journal of Colloid and Interface Scie*nce, **275**, 177 (2004).

5.J.S. Kim, E. Kuk, K.N Yu., J. H. Kim, S. J. Park, H. J. Lee, S.H. Kim., Y. K. Park., Y. H. Park., C.Y. Hwang, Y. K. Kim, YS. Lee, D.H. Jeong, MH. Cho, *Nanomedicin: Nanotechnology, Biology and medicine*; **1**, 95, (2007).

6.E. A. El-Sawi, M. A. Hosny, T. M. Sayed, *International Journal of Engineering Research and Technology* (IJERT), **3** (5): 770 (2014).

7.G. Madhu, K. Jayaveera, L. Ravindra, B. Kumar and P. Reddy, *Der Pharma Chemica*, **4 (**3), 1033 (2012).

8.K. Kaur, M. Jain, R. Reddy and R. Jain, *European Journal of Medicinal Chemistry,***45** (8), 3245 (2010).

9.A. Abadi, G. Hegazy and A. El-Zaher, *Biorganic and Medicinal Chemistry* **13**, 5759 (2005).

10. A. Abu-Hashem and A. Aly , *Arch Pharm Res*, **35** (3), 437 (2012).

11. L. Korrichi, B. Dalila and S.Dalila, *European Journal of biological Sciences*, **1** (3), 32 (2009).

12. L. Chen, I. Chen, C.Huang, C. Liao, C.Chen and T.Wang, *Journal of the Chinese Chemical Society*, **57**, 1331 (2010).

13. H. Hassanin, M. Ibrahim and Y.Alnamer, *Turkish Journal of Chemistry,* **36,** 682 (2012).

14. A. B. Ahvale , H. Prokopcova, J. Sefoviova , W. Steinschifter, A. E.Taubl, G.Uray, W. Stadlbauer, *Eur. J. Org. Chem*., 563 (2008).

15. I. V. Ukrainets, A. A. Tkach and L. Y.Yang, *Chem. Heterocycl.Compds*., **44**, 1347 (2008).

16. M.S. Mostafa, *Chemistry and Materials Research*, **3** (9):125 (2013).

17. E. A. El-Sawi, M. A. Hosny, W. A. Mokbel, T. M Sayed., *Synth. React. Inorg. Met. Nano- Met. Chem*., **40**, 934 (2010).

18. E. A. El-Sawi , W. A. Mokbel and T. M. Sayed, *Bulg. Chem. Commun*., **39**, 281 (2007).

19. E. A El-Sawi .and T. M. Sayed, *Synth. React. Inorg. Met.-Org. Nano- Met.Chem*, **41**,992 (2011).

20. D. H. Williams, I. Fleming,*Spectroscopic methods in organic chemistry*,2 nd. edition, McGraw-Hill Book Company(UK) limited, 1993, p. 1348.
21. E. Jawetz, J. L. Melnick, E. A. Adelberg, *Review of Medical. Microbiology, 14th ed, Lange Medical Publication, Los. Altos*, CA, 1980, p 45.
22. D. N. Muanza, B. W. Kim, L. L. Euler, L. Williams, *Int. J. Pharmacog.*, **32**, 337 (1994).
23. O. N. Irob, M.moo-Young, W. A. Aperson, *Inter. J. Pharmacol*., **34**, 87 (1996).
24. A. Sileikaite, I. Prosycevas, J. Puiso, A. Juraitis and A. Guobienė, *Material Science,* **12**, 1320 (2006).
25. M. Sastry, K. S Mayya, K. Bandyopadhyay, *Colloid. Surf.* A, 127-221 (1997).
26. M. Sastry, V. Patil.and S. R. Sainkar, *J Phys Chem B.* **102**, 1404 (1998).
27. V. Vichai and K. Kirtikara, *Sulforhodamine B colorimetric assay for cytotoxicity screening*., **1**, 1112 (2006)
A. Henglein, *J. Phys. Chem.* **97**, 5457 (1993).

СРЕБЪРНИ НАНОЧАСТИЦИ С НОВИ ОРГАНОМЕТАЛНИ СЪЕДИНЕНИЯ ПОДОБРЯВАТ АНТИМИКРОБНАТА АКТИВНОСТ

Е. А. Ел-Сауи[*], М. А. Хосни

Департамент по химия, Девически факултет по изкуства, наука и образование

Университет Ейн Шамс Хелиополис, Кайро, Египет

Постъпила на 6 януари, 2015 г., коригирана на 30 юли, 2015 г.

(Резюме)

Металираните хетероциклени съединения (4-9), получени при реакцията на 2-(2-оксо-2*H*-пирано[3,2-*h*] хинолин-4-ил) оцетна киселина (1) с 4-(2,2-дихидрокси-винил)-2*H*-пирано[3,2-*h*] хинолин-2-он (2) и техни производни (3) с ацетати на Co(II) и Cu(II). Изясняването на структурите им е направено с помощта на елементен анализ, IR, ^{1}HNMR и MS. Приготвените сребърни наночастици са изучени с трансмисионна електронна микроскопия (TEM) и UV-спектри. Изследвана е антимикробната активност на всички продукти, дотирани със сребърни наночастици спрямо основните съединения. Резултатите показват, че наночастиците повишават тази активност с 12-170% и може да се използват като инхибитори на растежа.на микроорганизмите